Superlattices and Microstructures 104 (2017) 308–315

Contents lists available at ScienceDirect

Superlattices and Microstructures

journal homepage: www.elsevier.com/locate/superlattices

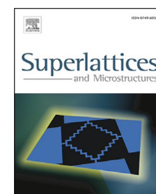

Ge nanocrystals embedded in ultrathin Si_3N_4 multilayers with SiO_2 barriers

R. Bahariqushchi [a,*], Sinan Gundogdu [a], A. Aydinli [b,1]

[a] Bilkent University, Physics Department, Ankara, 06800, Turkey

[b] Uludag University, Electrical and Electronics Engineering Department, Bursa, 16059, Turkey

ARTICLE INFO

Article history:
Received 17 January 2017
Received in revised form 20 February 2017
Accepted 21 February 2017
Available online 22 February 2017

ABSTRACT

Multilayers of germanium nanocrystals (NCs) embedded in thin films of silicon nitride matrix separated with SiO_2 barriers have been fabricated using plasma enhanced chemical vapor deposition (PECVD). SiGeN/SiO_2 alternating bilayers have been grown on quartz and Si substrates followed by post annealing in Ar ambient from 600 to 900 °C. High resolution transmission electron microscopy (HRTEM) as well as Raman spectroscopy show good crystallinity of Ge confined to SiGeN layers in samples annealed at 900 °C. Strong compressive stress for SiGeN/SiO_2 structures were observed through Raman spectroscopy. Size, as well as NC-NC distance were controlled along the growth direction for multilayer samples by varying the thickness of bilayers. Visible photoluminescence (PL) at 2.3 and 3.1 eV with NC size dependent intensity is observed and possible origin of PL is discussed.

© 2017 Elsevier Ltd. All rights reserved.

1. Introduction

Silicon and germanium nanocrystals (NCs) embedded in a dielectric matrix such as SiO_2, Al_2O_3 and Si_3N_4 have been shown to have potential in optoelectronic, photovoltaic and memory device applications [1–3]. Despite some successful implementations, problems remain that hinder the broadening of applications. Amongst them are the random nature of size and distribution of NCs [4–6] as well as their inability to conduct electrical current when embedded in a dielectric media [7]. Control of size and distribution could help pave the way for useful embedded architectures that exploit the quantum nature of the NCs invoking topologies amenable to diffusion. One approach is to employ semiconductor rich thin dielectric layers separated with undoped dielectric barriers to limit the size of crystal growth during subsequent annealing. This may also make it possible to build three dimensional NC scaffolds that channel energy whether by light or by carrier using multilayers of NCs in various dielectrics. Previously, multilayers of Si and Ge NCs embedded in SiO_2 and Al_2O_3 have been fabricated using magnetron sputtering [6,8–11] where control over size as well as concentration over NCs was shown. PL enhancement in SiO_2:Ge NC multilayer samples is also reported [12].

Ge has larger excitonic Bohr radius (24.3 nm) compared to that of Si (4.9 nm) [4] due to its smaller electron and hole effective masses and larger dielectric constant. Therefore, quantum confiement effect can be seen even in larger Ge NCs and it would be easier to tune electrical and optical properties of Ge by controlling the size of NCs. In Ge, with small energy difference between direct and indirect band gaps, radiative recombination occurs more rapidly compared to Si. Ge also has

* Corresponding author.
E-mail address: rahim.qushchi@fen.bilkent.edu.tr (R. Bahariqushchi).

[1] Formerly at Bilkent University, Physics Department, Ankara, 06800, Turkey.

http://dx.doi.org/10.1016/j.spmi.2017.02.037
0749-6036/© 2017 Elsevier Ltd. All rights reserved.

melting point of 938 °C which is lower than that of Si (1414 °C), suggesting that Ge NCs can be fabricated at lower temperatures which reduces cost of manufacturing. Moreover, fabrication of NCs inside SiO_2 or Al_2O_3 matrices is associated with oxidation of NCs [13,14]. Large barrier heights in SiO_2 and Al_2O_3 matrices also leads to reduction of charge transport [14]. Si_3N_4, used as a host matrix is a good candidate to overcome these problems. Despite the intense study of Ge NCs in SiO_2 matrix, there are few reports [15–17] on Ge NCs embedded in Si_3N_4 matrices, yet fewer of its multilayers. In this paper, we report on a study of Ge NCs embedded in Si_3N_4 matrix in multilayer structures deposited using plasma enhanced chemical vapor deposition, (PECVD). Several techniques such as co-sputtering [4], ion implantation [18], anodic etching [19], cluster beam method [20] have previously been used to prepare Ge NCs in SiO_2 matrices. PECVD has some advantages over other methods such as lower process temperature, high blocking effects against moisture and alkaline ions, high dielectric constant. In contrast with Ge NCs prepared by magnetron sputtering [15], it has been shown that Ge/oxide interface in samples prepared by PECVD is much sharper [21] which can lead to better tuning of optical and electrical properties in PECVD samples.

Here, we studied the structural and optical properties of Ge NCs embedded in thin Si_3N_4 layers with SiO_2 barriers in SiGeN:SiO_2 multilayer structures using TEM, Raman and photoluminescence (PL) spectroscopy. Multilayer structures have several advantages over single layer samples, where Ge content in as-grown samples is central in the determination of nanocrystal sizes. Typically, NC size is controlled by annealing temperature and duration or the content of the relevant material in the dielectric matrix [22] when annealed at fixed temperatures. In single layers, size of small Ge NCs are limited by the amount of Ge in SiN_x which leads to low density of nanocrystals that reduces photoluminescence efficiency. Multilayer approach can overcome this problem by controlling the size of NCs by confining them in thin layers and by increasing the number of Ge containing layers. Here, we separate adjacent layers of Ge containing nitride layers with dielectric barriers such as SiO_2 which is expected to prevent Ge cross diffusion during annealing and therefore, can lead to small NCs with high concentration. This allows the controlling of the size and density of NCs, simultaneously. Moreover this approach, provides the local control of NCs and NC-NC distance in the growth direction.

2. Experiment

Multilayer samples with successive bilayers of SiGeN/SiO_2 up to eight bilayers have been prepared. SiO_2 layers are expected to act as barriers for Ge diffusion and control the NC-to-NC distance along the growth direction. Growths have been done in a PECVD reactor (model PLASMALab 8510C) on quartz and Si substrates. For growing SiGeN films, we used 100 sccm SiH_4 (2% in N_2), 30 sccm NH_3 and 200 sccm GeH_4 (2% in He). For SiO_2 barriers, 50 sccm SiH_4(2% in N_2) and 1000 sccm N_2O is used. The process pressure was 1000 mbar, RF power was 12 W and sample temperature was 250 °C. We fabricated several samples with SiO_2 barrier thickness of 25 nm and SiGeN thickness of 3, 6 and 9 nm. The samples are labeled as ML3, ML6 and ML9 where the numbers indicate the thickness of SiGeN films thickness in nanometers, respectively. The samples are annealed under Ar ambient from 600 °C to 900 °C for 30 min. The structural characterization of samples were performed using a 300 KV TECNAI f30 field emission transmission electron microscope. Samples for TEM study were prepared with a focus ion beam tool with Ga+ as the ion beam. At the final stages of the sample preparation, Ga+ beam energy was lowered for final polishing of the surfaces. Raman spectroscopy was done with a cw Ar^+ laser operating at 514 nm using a 1 m double grating monochromator with high resolution and a cooled CCD camera. PL spectroscopy have been done using a HeCd laser operating at 325 nm on the same system.

3. Results and discussion

The structure of samples with different SiGeN thickness were observed using high resolution transmission electron microscopy (HRTEM) after annealing them up to 900 °C for 30 min. Fig. 1 shows overall TEM micrographs for all three samples with differing thicknesses of SiGeN layer annealed at 850–900 °C. Samples with 3, 6 and 9 nm thick SiGeN layers show similar behaviours, albeit some differences, Fig. 1a–c, respectively. The periodicity of the SiO_2 barrier is the same in all samples and we clearly see the clustering and crystallisation of Ge in the SiGeN layers in all three samples. It is also clear that while there is no diffusion of Ge atoms from layer to layer, lateral diffusion of Ge in the SiGeN plane is accompanied in thicker SiGeN layers with vertical growth of the nanocrystals leading to ellipsoidal shapes in an effort to minimize the surface free energy which is minimum for spheres [23]. Lateral diffusion of Ge and subsequent ellipsoidal growth leads to bead like formations modulating the NC sizes. We note that the sizes of the Ge NCs along the growth direction are larger as the thickness of SiGeN layer increases. This would lead to variations in the effective band gap of the NCs as well as creating bottlenecks in carrier transport. On the other hand, it may present opportunities to create controlled three dimensional growth of nano-Ge lattices. It is clear from the TEM micrographs that the driving force for the ultimate spherical shape is large enough that some diffusion into SiO_2 barriers takes place. The extend of the diffusion increases with the thickness of the Ge containing SiGeN layer due to available Ge atoms. Thinner layers do not contain enough Ge atoms to support the drive to spherical shapes. As the amount of Ge in SiGeN layers increase, while not observed here, vertical diffusion accompanying the lateral crystallisation may be expected to increase, reaching to a point that Ge NC layers touch each other.

Close up TEM micrographs are shown in Fig. 2 starting with a) sample ML3 (multilayer with nominal 3 nm SiGeN) sample with the thinnest SiGeN layer. The SiO_2 barrier thickness of 25 nm is observed along with the diffused Ge in layers between the barriers. The in-plane diffusion of Ge atoms leads to thickening of the Ge layer and buckling of the Ge NCs where some parts of the Ge NCs is thicker with periodicity of around 25 nm. We note that, Ge diffusion perpendicular to the Ge NCs is

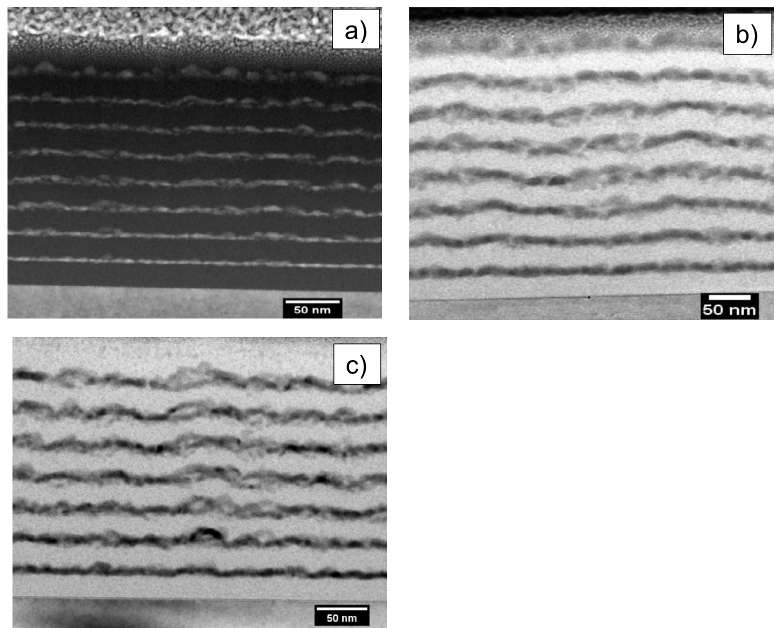

Fig. 1. TEM micrographs of samples with SiGeN thicknesses and annealing temperatures of samples with a) 3 nm (900 °C), b) 6 nm (850 °C) and c) 9 nm (900 °C). The barriers are SiO_2 with thickness of 25 nm.

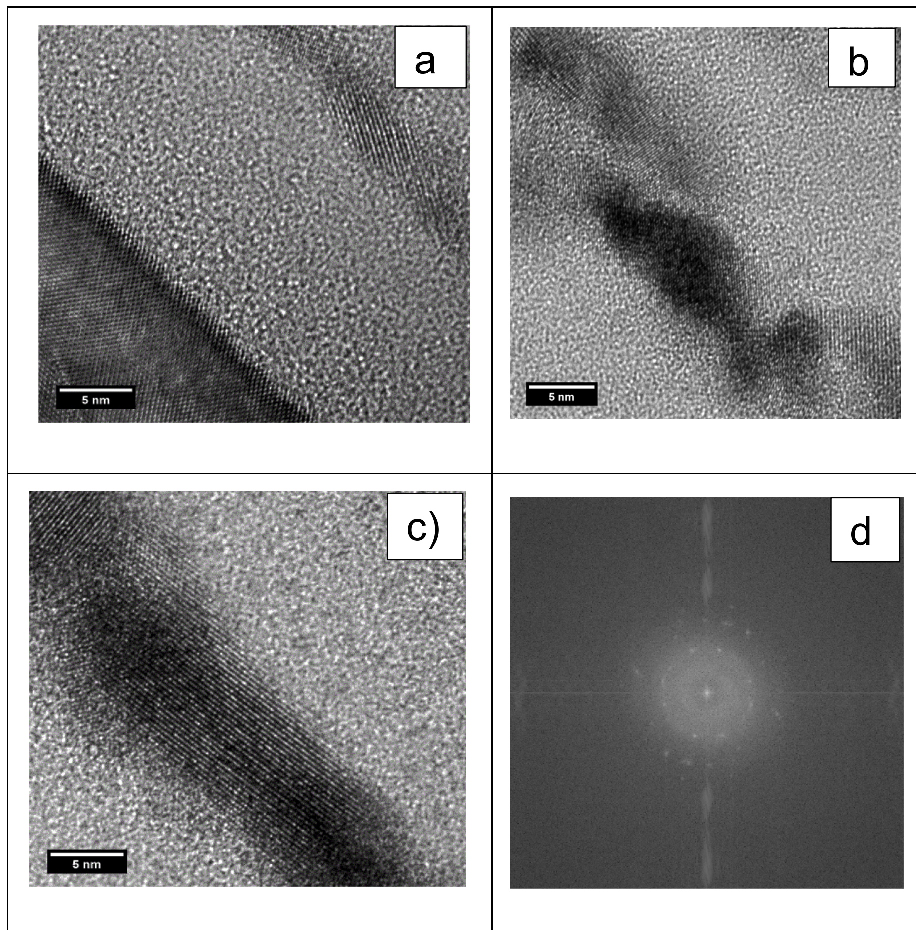

Fig. 2. Cross-section TEM and typical FFT micrograph of multilayer samples: (a),(b),(c) HRTEM graphs of samples with 3, 6 and 9 nm of SiGeN layers, respectively.(d) FFT micrograph of sample (c) The graphs show good crystallinity as well as control over size by multilayer approach.

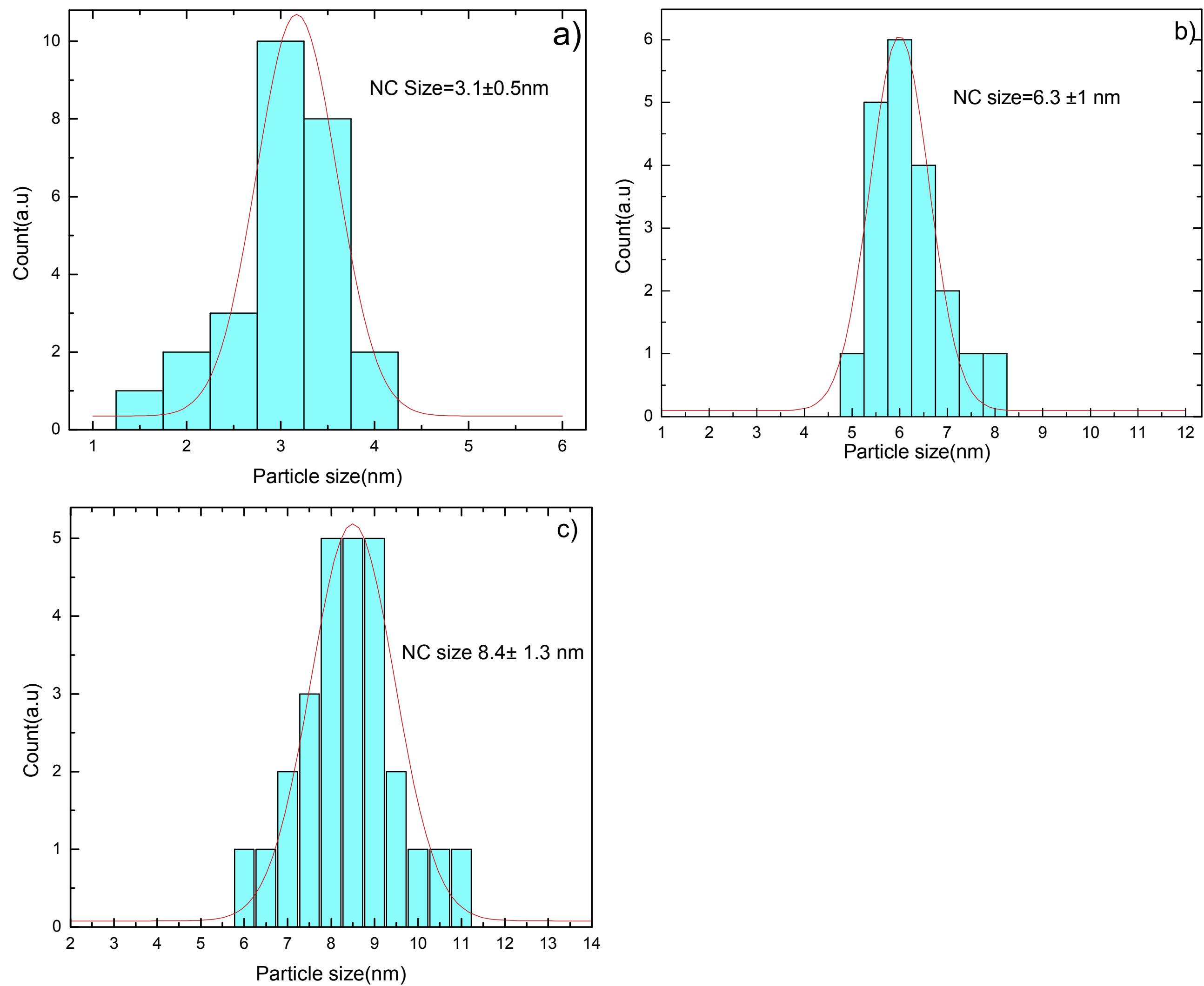

Fig. 3. Size distribution for multilayer structures with different thicknesses and related Gaussian fit. It is clear that size of NCs is mostly determined by the thickness of the SiGeN layer thickness. The size distribution is narrow in all three samples.

limited by the lateral in plane diffusion of Ge atoms such that the size of NCs is expected to be restricted by the thickness of SiGeN films [12]. In single bulk-like layers, NCs are typically spherical in shape [23] since minimum surface to volume ratio for spherical geometry leads to minimisation of interface energy for spherical NCs. Spherical NCs are, therefore, expected. However, these HRTEM micrographs show confinement of Ge along the growth direction and in plane growth of small Ge NCs in thin SiGeN layers and lateral growth of elongated Ge NCs for thicker samples. As shown in these images, in all samples, our SiGeN layers have wavy shape with smoother interfaces at layers closer to substrate. This behavior is reported in several works [24–26]. Theoretical calculations also have been done [27] and predicted flatter and sharper interfaces at layers closer to substrate. In Ref. [24] also much smoother interfaces are observed in the as-grown samples compared to annealed samples. This has been attributed to interlayer diffusion of Ge confirmed by RBS study of Ge content. However, in our case, the as-grown samples (not shown here) show the same wavy structure as annealed samples. It seems that the effect of Ge diffusion during annealing plays a limited role in the formation of the wavy structure. We have not observed a Ge diffusion channel between Ge rich layers under the conditions of our experiments. Our as-grown samples are similar to samples in Ref. [26] where the origin of wavy structure in as-grown samples is attributed to insufficient energy of arriving atoms to make atomic rearrangement upon surface adsorption. The arriving atoms stick where they land. The exact shape of the interface depends on deposition conditions. Then the small intrinsic waviness in initial layers of a multilayer system leads to a large cumulative waviness towards top of the system. We also suggest this is the possible responsible mechanism of waviness in our samples.

Fig. 3 shows size distribution for these three samples with different thicknesses. The NC size is referred to here is the NC diameter in the growth direction which is controlled via SiGeN thickness.

Raman spectroscopy is a very useful technique to study crystalline structures, size distribution and film stress. Fig. 4 shows the Raman spectra for as-grown and annealed samples. The spectra shows phase transition from amorphous to crystalline as a function of annealing temperature. For as-grown samples a broad spectra around 277 cm^{-1} is observed which is related to the amorphous Ge phase [28,29]. All annealed samples have sharp peaks around 300 cm^{-1}. They show small blueshift with respect to bulk germanium at 300.7 cm^{-1} [30]. Raman peaks do not show a red shift as expected from phonon confinement model, instead show a blue shift which can be due to compressive stress induced by the matrix [31–33]. The compressive stress induced blue shift is reduced by the red shift due to phonon confinement which is more pronounced for smaller NCs. Therefore, Raman shifts for smaller Ge NCs (samples annealed at lower temperatures) is at lower wavenumbers compared to samples with larger NCs (annealed at higher temperatures) which is due to phonon confinement effect. To summarize, total Raman peak shift can be divided in two main parts: Redshift due to phonon confinement effect, which is dominant for smaller NCs and compressive stress induced blue shift, which normally is stronger for smaller NCs. On the other hand, for the small particles stress can be considered to be constant for all samples [21,22] with the observed Raman shift being attributed to phonon confinement only. As is observed in the TEM micrographs, thickness of SiGeN films, dictates the average size of Ge NCs and samples with thinner SiGeN layers have Raman peak at higher wave numbers, as expected from phonon confinement effect. We also observe that the intensity of Raman signal increases as the thickness (and therefore average NCs size) increases. This is due to larger Ge NCs in these samples. Also the width of the Raman peaks (FWHM) increases from 5.2 cm^{-1} to 11.2 cm^{-1}, 9.8 cm^{-1} and 8.1 cm^{-1} for ML3, ML6 and ML9 samples, respectively, i.e: broader spectra for smaller NCs. Also an asymmetry is observed at lower wavenumber side of the spectra.

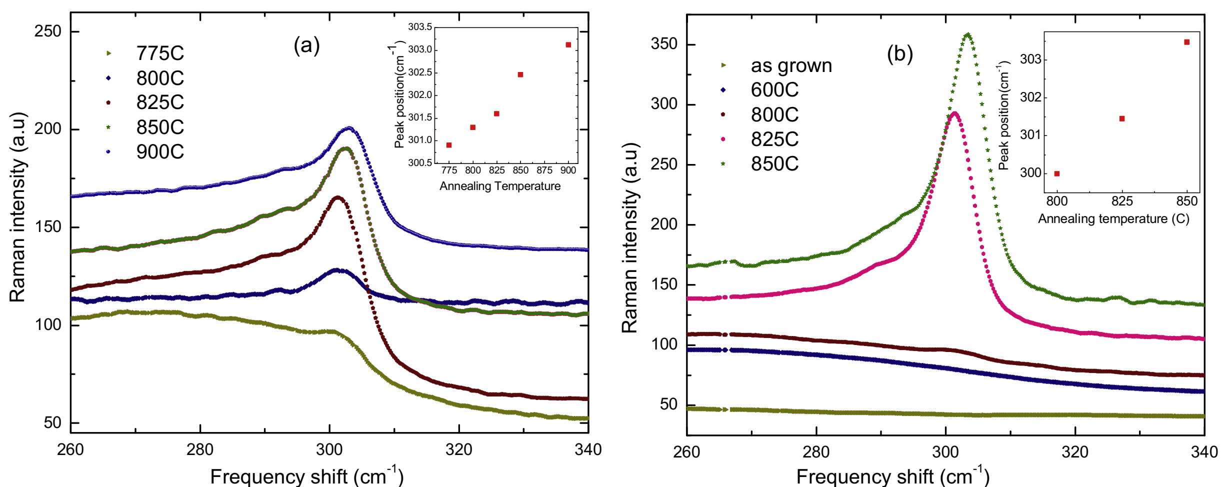

Fig. 4. Raman spectra for ML3 (a) and ML6 (b) using the 514 nm line of an Ar+ laser showing the onset of crystallisation and the subsequent blue shift. Crystallisation threshold is 775 °C for a 30 min anneal. Insets show Raman peak position as a function of annealing temperature. (For interpretation of the references to colour in this figure legend, the reader is referred to the web version of this article.)

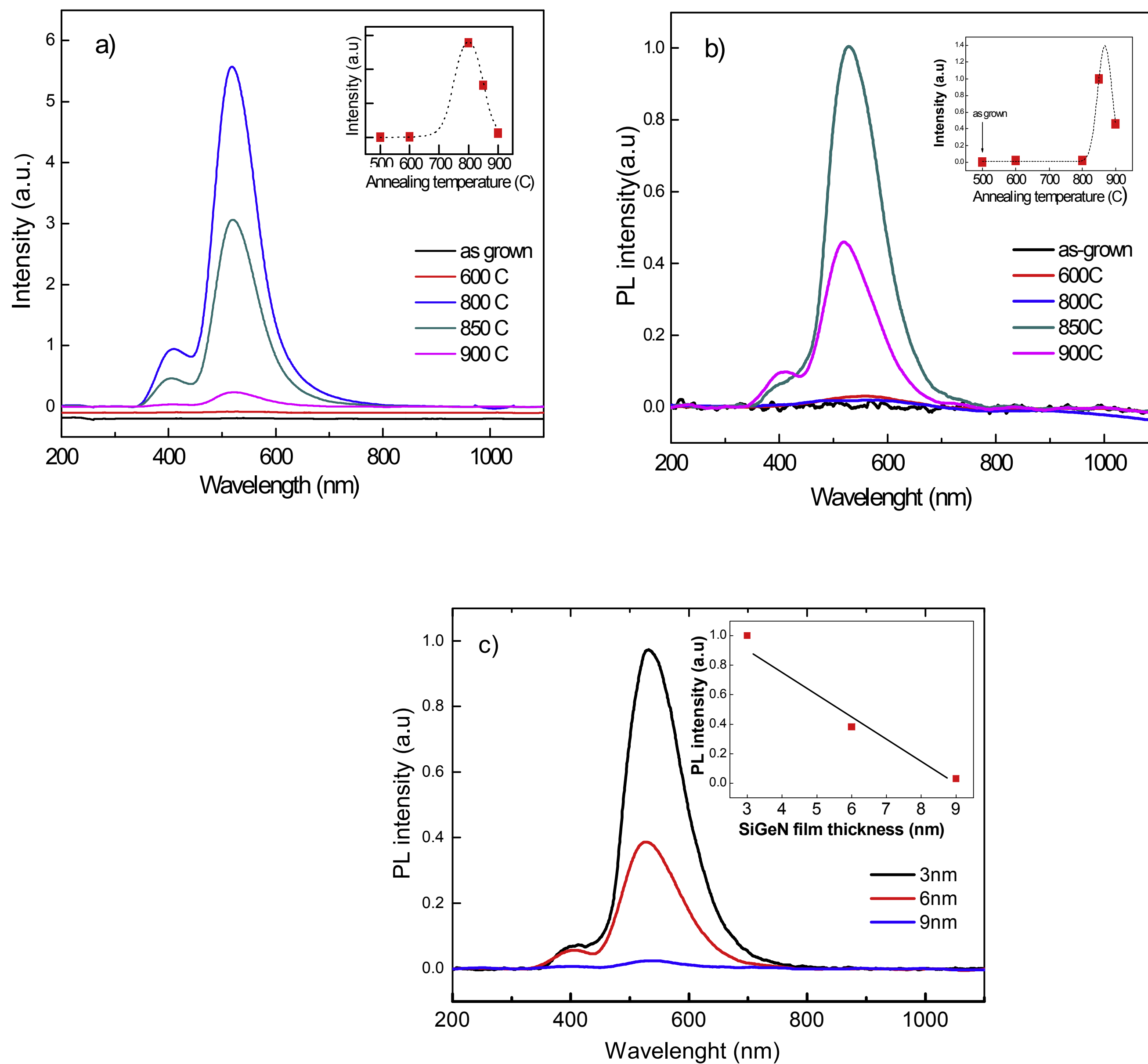

Fig. 5. PL spectra of samples a) ML3 and b) ML6 annealed at different temperatures c) Comparison of PL intensity of samples ML3, ML6 and ML9 annealed at 900 °C. The inset shows a plot of PL intensity versus NC size. We note that PL spectra intensity is enhanced with reduction of NCs size. Insets in a) and b) show the variation of PL intensity as a function of annealing temperature while c) shows variation of Pl intensity with NC size.

We also performed photoluminescence measurements on these samples to investigate their optical properties. Fig. 5 shows the photoluminescence spectra of samples ML3, ML6 and ML9. at room temperature. The photoluminescence peak position does not show observable shift with annealing temperature. However, we observe a size-dependent photoluminescence intensity. We note that, the highest photoluminescence intensity of NCs of 3.1 nm decreases as the NC size increases to 6.4 nm finally decreasing to zero when the quantum size is 9.0 nm. Visible photoluminescence in Ge NCs was observed for the first time by Maeda et al. [4] they attributed the origin of their PL to confinement effect, however they did not show peak shift with changing NC size. Zacharias et al. [34] also observed visible PL from Ge NCs and also did not observe the confinement effect. They related the PL to defects in matrix. The first PL attributed to QCE was observed by Takeoka et al. [35] in 1998. They observed a blue peak shift with changing Ge NC size. Despite the later works [32–37] on Ge NCs in different matrices and different NC preparation methods, there is no agreement on the origin of PL in Ge NCs. Up to our knowledge the report by Takeoka [35] is the only PL observation of embedded Ge in consistent with QCE. Theses inconsistencies arise from ill-defined surface chemistry and complex-defective interfaces between Ge NCs and the surrounding matrix [35]. These surface related effects makes the observation of QCE more challenging in Ge NCs compare to Si NCs. Generally the PL from films containing Ge NCs is attributed to three effects: First, it can originate from quantum confinement of electrons and holes inside NCs. This inevitably leads to the expectation that a size dependent shift of the luminescence wavelength [4,12,34,37,38] should be observed. This is not the case for our samples. Since the PL spectra shows no peak shift with NCs size in our samples, this possibility is ruled out. Second, photoluminescence may also be observed in samples with matrix defects [17,30] which are created during film growth or diffusion of Ge during annealing. This is not also the case for our samples. We do not observe PL in as-grown samples, so that defect originated during sample growth, does not seem to be a possibility. Also, the defects due to diffusion of Ge during annealing is expected to be present in all samples including samples with 9.0 nm NCs. However these samples also show no PL. We, therefore, conclude that matrix defects is not considered to be the origin of PL in our samples. The third possibility is PL due to states related to the interface of NC-dielectric matrix. Besides QCE, decreasing the size of NCs, cause a notable increase of surface to volume ratio of Ge NCs, which in turn, increases surface related effects. We believe this is the most likely origin of PL in our samples. This is supported by the fact that PL intensity is correlated with crystallisation of Ge and with the size of Ge NCs. Raman and PL data for samples with 3 and 6 nm SiGeN films show that PL emission threshold is associated with beginning of crystallisation of Ge. PL emission is observed when crystallisation becomes apparent in the Raman spectra. Even though there is no peak shift as the NCs size changes, there is a strong dependence of PL intensity on NCs size. These results show that the PL signal is related to small NCs as small as 6 nm or less while we do not observe PL from samples with NC size of 9 nm or larger. This can be due to larger number of surface effects at smaller Ge NCs since they have larger surface to volume ratio. This is in agreement with results of Maeda et al. [4] and Barbagiovanni [39] who observed strong visible PL originating from interface states of very small Ge NCs.

4. Conclusions

We performed an experimental investigation on the synthesis, optical and structural properties of Ge NCs embedded in Si_3N_4 matrix prepared by PECVD. SiGeN layers are separated by SiO_2 barriers. Thermal annealing in Ar ambient up to 900 °C for 30 min have been done to induce crystallisation. Multilayers of SiGeN/SiO_2 bilayers are used to control NC size as well as NC-NC distance in growth direction and concentration of NCs. Raman spectroscopy and HRTEM graphs show crystallisation of samples annealed at 800 °C and higher temperatures. NC sizes are tuned between 3 nm and 9nm which are dictated by SiGeN film thicknesses. Compressive stress on Ge NCs in silicon nitride matrix is identified with the observation of blueshift in the Raman spectra of samples. Photoluminescence study have been done using HeCd laser performing at 325 nm. We observed a size dependent PL intensity at 2.3 and 3.1eV. The samples with NCs below or equal to 6 nm show visible PL. We observed the enhancement of the PL intensity with reduction of the NCs size. The reduction of NC size is accompanied with increasing surface to volume ratio and therefore increasing surface related states.The origin of PL is suggested to be due to recombination through states at the NC/matrix interface.

Acknowledgments

The authors acknowledge use of the services and facilities of UNAM-National Nanotechnology Research Center at Bilkent University.

References

[1] Robert J. Walters, George I. Bourianoff, Harry A. Atwater, Field-effect electroluminescence in silicon nanocrystals, Nat. Mater. 4 (2) (2005) 143–146.
[2] Gavin Conibeer, Martin Green, Richard Corkish, Young Cho, Eun-Chel Cho, Chu-Wei Jiang, Thipwan Fangsuwannarak, et al., Silicon nanostructures for third generation photovoltaic solar cells, Thin Solid Films 511 (2006) 654–662.
[3] Aykutlu Dâna, Imran Akca, Atilla Aydinli, Rasit Turan, Terje G. Finstad, A figure of merit for optimization of nanocrystal flash memory design, J. Nanosci. Nanotechnol. 8 (2) (2008) 510–517.
[4] Yoshihito Maeda, Nobuo Tsukamoto, Yoshiaki Yazawa, Yoshihiko Kanemitsu, Yasuaki Masumoto, Visible photoluminescence of Ge microcrystals embedded in SiO2 glassy matrices, Appl. Phys. Lett. 59 (24) (1991) 3168–3170.
[5] A. Kanjilal, J. Lundsgaard Hansen, P. Gaiduk, A. Nylandsted Larsen, N. Cherkashin, A. Claverie, P. Normand, E. Kapelanakis, D. Skarlatos, D. Tsoukalas, Structural and electrical properties of silicon dioxide layers with embedded germanium nanocrystals grown by molecular beam epitaxy, Appl. Phys. Lett. 82 (8) (2003) 1212–1214.

[6] H.G. Chew, F. Zheng, W.K. Choi, W.K. Chim, Y.L. Foo, E.A. Fitzgerald, "Influence of reductant and germanium concentration on the growth and stress development of germanium nanocrystals in silicon oxide matrix, Nanotechnology 18 (6) (2007) 065302.
[7] Chu-Wei Jiang, Martin A. Green, Silicon quantum dot superlattices: modeling of energy bands, densities of states, and mobilities for silicon tandem solar cell applications, J. Appl. Phys. 99 (11) (2006) 114902.
[8] Gavin Conibeer, Martin Green, Eun-Chel Cho, Dirk König, Young-Hyun Cho, Thipwan Fangsuwannarak, Giuseppe Scardera, et al., Silicon quantum dot nanostructures for tandem photovoltaic cells, Thin Solid Films 516 (20) (2008) 6748–6756.
[9] Margit Zacharias, J. Heitmann, R. Scholz, U. Kahler, M. Schmidt, J. Bläsing, Size-controlled highly luminescent silicon nanocrystals: a SiO/SiO 2 superlattice approach, Appl. Phys. Lett. 80 (4) (2002) 661–663.
[10] Fei Gao, Martin A. Green, Gavin Conibeer, Eun-Chel Cho, Yidan Huang, Ivan Pere-Wurfl, Chris Flynn, Fabrication of multilayered Ge nanocrystals by magnetron sputtering and annealing, Nanotechnology 19 (45) (2008) 455611.
[11] M. Ardyanian, H. Rinnert, M. Vergnat, Structure and photoluminescence properties of evaporated Ge O x∕ Si O 2 multilayers, J. Appl. Phys. 100 (11) (2006) 113106.
[12] J.K. Shen, X.L. Wu, R.K. Yuan, N. Tang, J.P. Zou, Y.F. Mei, C. Tan, X.M. Bao, G.G. Siu, Enhanced ultraviolet photoluminescence from SiO 2/Ge: SiO 2/SiO 2 sandwiched structure, Appl. Phys. Lett. 77 (20) (2000) 3134–3136.
[13] K.L. Teo, S.H. Kwok, P.Y. Yu, Soumyendu Guha, Quantum confinement of quasi-two-dimensional E 1 excitons in Ge nanocrystals studied by resonant Raman scattering, Phys. Rev. B 62 (3) (2000) 1584.
[14] E.S. Marstein, A.E. Gunnæs, U. Serincan, S. Jørgensen, A. Olsen, R. Turan, T.G. Finstad, "Mechanisms of void formation in Ge implanted SiO 2 films, Nucl. Instrum. Methods Phys. Res. Sect. B Beam Interact. Mater. Atoms 207 (4) (2003) 424–433.
[15] S. Mirabella, S. Cosentino, A. Gentile, G. Nicotra, N. Piluso, L.V. Mercaldo, F. Simone, C. Spinella, A. Terrasi, Matrix role in Ge nanoclusters embedded in Si3N4 or SiO2, Appl. Phys. Lett. 101 (1) (2012) 011911.
[16] S. Mirabella, S. Cosentino, A. Gentile, G. Nicotra, N. Piluso, L.V. Mercaldo, F. Simone, C. Spinella, A. Terrasi, Matrix role in Ge nanoclusters embedded in Si3N4 or SiO2, Appl. Phys. Lett. 101 (1) (2012) 011911.
[17] Aykutlu Dana, Serkan Tokay, Atilla Aydinli, Formation of Ge nanocrystals and SiGe in PECVD grown SiNx: Ge thin films, Mater. Sci. Semicond. Process. 9 (4) (2006) 848–852.
[18] M. Zacharias, J. Bläsing, J. Christen, P. Veit, B. Dietrich, D. Bimberg, Formation of Ge nanocrystals with sharp size distribution: structural and optical characterization, Superlattices Microstruct. 18 (2) (1995) 139–146.
[19] Leigh T. Canham, Silicon quantum wire array fabrication by electrochemical and chemical dissolution of wafers, Appl. Phys. Lett. 57 (10) (1990) 1046–1048.
[20] M. Ehbrecht, B. Kohn, F. Huisken, M.A. Laguna, V. Paillard, Photoluminescence and resonant Raman spectra of silicon films produced by size-selected cluster beam deposition, Phys. Rev. B 56 (11) (1997) 6958.
[21] S. Cosentino, A.M. Mio, E.G. Barbagiovanni, R. Raciti, R. Bahariqushchi, M. Miritello, G. Nicotra, et al., The role of the interface in germanium quantum dots: when not only size matters for quantum confinement effects, Nanoscale 7 (26) (2015) 11401–11408.
[22] A. Wellner, V. Paillard, C. Bonafos, H. Coffin, A. Claverie, B. Schmidt, K.H. Heinig, Stress measurements of germanium nanocrystals embedded in silicon oxide, J. Appl. Phys. 94 (9) (2003) 5639–5642.
[23] D.M. Sagar, Joanna M. Atkin, Peter KB Palomaki, Nathan R. Neale, Jeffrey L. Blackburn, Justin C. Johnson, Arthur J. Nozik, Markus B. Raschke, Matthew C. Beard, Quantum confined electron–phonon interaction in silicon nanocrystals, Nano Lett. 15 (3) (2015) 1511–1516.
[24] E.M.F. Vieira, J. Martín-Sánchez, Anabela G. Rolo, Andrea Parisini, Maja Buljan, I. Capan, Eduardo Alves, et al., Structural and electrical studies of ultrathin layers with Si0. 7Ge0. 3 nanocrystals confined in a SiGe/SiO2 superlattice, J. Appl. Phys. 111 (10) (2012) 104323.
[25] Stephen P. Vernon, Daniel G. Stearns, Robert S. Rosen, Ion-assisted sputter deposition of molybdenum-silicon multilayers, Appl. Opt. 32 (34) (1993) 6969–6974.
[26] Andreas Kling, A. Rodriguez, J. Sangrador, M.I. Ortiz, T. Rodriguez, C. Ballesteros, J.C. Soares, Combined grazing incidence RBS and TEM analysis of luminescent nano-SiGe/SiO 2 multilayers, Nucl. Instrum. Methods Phys. Res. Sect. B Beam Interact. Mater. Atoms 266 (8) (2008) 1397–1401.
[27] A.P. Payne, B.M. Clemens, Influence of roughness distributions and correlations on x-ray diffraction from superlattices, Phys. Rev. B 47 (4) (1993) 2289.
[28] P.H. Tan, K. Brunner, Dominique Bougeard, Gerhard Abstreiter, Raman characterization of strain and composition in small-sized self-assembled Si/Ge dots, Phys. Rev. B 68 (12) (2003) 125302.
[29] Aycan Yurtsever, Matthew Weyland, D. Muller, 3-D imaging of non-spherical silicon nanoparticles embedded in silicon oxide by plasmon tomography, Microsc. Microanal. 12 (S02) (2006) 532–533.
[30] Po-Hsiang Liao, Ting-Chia Hsu, Kuan-Hung Chen, Tzu-Hsuan Cheng, Tzu-Min Hsu, Ching-Chi Wang, Tom George, P.W. Li, Size-tunable strain engineering in Ge nanocrystals embedded within SiO2 and Si3N4, Appl. Phys. Lett. 105 (17) (2014) 172106. Wellner, A., V. Paillard, C. Bonafos, H. Coffin, A. Claverie, B. Schmidt, and K. H. Heinig. "Stress measurements of germanium nanocrystals embedded in silicon oxide." Journal of applied physics 94, no. 9(2003): 5639–5642.
[31] Oded Millo, Isacc Balberg, Doron Azulay, Tapas K. Purkait, Anindya K. Swarnakar, Eric Rivard, Jonathan GC. Veinot, Direct evaluation of the quantum confinement effect in single isolated Ge nanocrystals, J. Phys. Chem. Lett. 6 (17) (2015) 3396–3402.
[32] Yoshihiko Kanemitsu, Hiroshi Uto, Yasuaki Masumoto, Yoshihito Maeda, On the origin of visible photoluminescence in nanometer-size Ge crystallites, Appl. Phys. Lett. 61 (18) (1992) 2187–2189.
[33] Shinji Okamoto, Yoshihiko Kanemitsu, Photoluminescence properties of surface-oxidized Ge nanocrystals: surface localization of excitons, Phys. Rev. B 54 (23) (1996) 16421.
[34] M. Zacharias, P.M. Fauchet, Blue luminescence in films containing Ge and GeO 2 nanocrystals: the role of defects, Appl. Phys. Lett. 71 (3) (1997) 380–382.
[35] Shinji Takeoka, Minoru Fujii, Shinji Hayashi, Keiichi Yamamoto, Size-dependent near-infrared photoluminescence from Ge nanocrystals embedded in SiO 2 matrices, Phys. Rev. B 58 (12) (1998) 7921.
[36] D.C. Paine, C. Caragianis, T.Y. Kim, Y. Shigesato, T. Ishahara, Visible photoluminescence from nanocrystalline Ge formed by H2 reduction of Si0. 6Ge0. 4O2, Appl. Phys. Lett. 62 (22) (1993) 2842–2844.
[37] Tapas K. Purkait, Anindya K. Swarnakar, B. Glenda, Frank A. Hegmann, Eric Rivard, Jonathan GC. Veinot, One-pot synthesis of functionalized germanium nanocrystals from a single source precursor, Nanoscale 7 (6) (2015) 2241–2244.
[38] Yoshihito Maeda, Visible photoluminescence from nanocrystallite Ge embedded in a glassy SiO 2 matrix: evidence in support of the quantum-confinement mechanism, Phys. Rev. B 51 (3) (1995) 1658.
[39] E.G. Barbagiovanni, D.J. Lockwood, N.L. Rowell, R.N. Costa Filho, I. Berbezier, G. Amiard, L. Favre, A. Ronda, M. Faustini, D. Grosso, Role of quantum confinement in luminescence efficiency of group IV nanostructures, J. Appl. Phys. 115 (4) (2014) 044311.